

Posthumous Analysis of the Indian Anti-Satellite Experiment Part III: A Plausible Fragmentation Scenario

Arjun Tan

*Department of Physics, Alabama A & M University,
Normal, AL 35762, U. S. A.*

Abstract

The Indian anti-satellite (ASAT) experiment of 27 March 2019 created several unexpected results. The most unusual amongst them was that the Gabbard diagram was that of four separate fragmentations, the first of its kind ever recorded. The primary fragmentation was caused by the hypervelocity impact of the ASAT, which was followed by three successive explosive fragmentations of the main remnant of the target satellite. The fragments produced by each breakup was characterized by its apogee and perigee lines of definite slopes. A theory of apsidal slopes is formulated which shows that the sum of the slopes of the apogee and perigee lines is a constant for fragmentation from any location in the same orbit. The slopes of the apsidal lines were calculated at various true anomalies of the fragmenting orbit and compared with the observed slopes. The true anomalies of the breakup locations were determined where the calculated values of the slopes matched the observed values. It was concluded without ambiguity that the explosions occurred at 1-minute intervals at true anomalies of 93° , 97° and 101° in the ascending phase in a remnant orbit, 0.12404 day or approximately two revolutions after the initial collision of the ASAT with its target. The dramatic increases in the size and ellipticity of the remnant orbit following the explosions support these findings.

1. INTRODUCTION

On 27 March 2019, *India became the fourth nation in history to attain anti-satellite (ASAT) capability* when its *Microsat-R* satellite was destroyed in Sun-synchronous orbit. The ASAT weapon was a kinetic kill vehicle (KKV) atop a third-stage rocket

launched from Abdul Kalam Island [1]. The impact occurred at 11:13 IST or 05:43 UT on Julian day 2019086 at epoch 2019086.23819444. The location of the event was over Bay of Bengal at 18.715°N latitude and 87.450°E longitude [2]. The mass of the target satellite was 740 kg whereas the third-stage rocket including the KKV weighed 1,800 kg [3]. The ASAT experiment was planned such that the fragments produced by the backward impulse would deorbit rapidly and pose no threat to the space environment. However, several hundreds of fragments spread in the forward direction, many of them into higher energy orbits. By the end of the year 2019, 348 fragments (excluding the main remnant of the parent satellite) were cataloged [4]. Analyses of this event showed that the breakup of the Microsat-R satellite was one of a unique kind never witnessed before [5, 6]. The **Gabbard diagram** of the fragments revealed that it comprised four distinct Gabbard diagrams belonging to four groups of fragments in one, each having its own apogee and perigee lines, which was possible only if four distinct fragmentations had taken place sequentially [5]. The slopes of the apsidal lines together with the epochs of the fragments first cataloged point to the following scenario: The **primary fragmentation** was caused by the **hypervelocity impact** of the KKV producing **Group 1 fragments**; which was followed by the **secondary, tertiary and quaternary fragmentations** caused by **explosions** in the main remnant of the target satellite in rapid successions, producing **fragment Groups 2, 3 and 4** [5]. Of the 348 cataloged fragments, 144 belonged to Group 1 and the rest 204 belonged to the latter groups [5]. The fragments of the latter groups were so tightly clustered together that numerical breakdown of them was not feasible. Figure 1 shows the composite Gabbard diagram with the apogee and perigee lines of the Group 1 fragments marked. Figure 2 shows only the Groups 2, 3 and 4 fragments with their respective apsidal lines, with the Group 1 fragments purged (for better clarity). The observed slopes of the apogee and perigee lines were calculated graphically and entered in Table I. In this paper, a theory of apsidal line slopes is formulated and compared with the observed slopes. The details of the sequence of four fragmentations are extracted from the results,

Table I. Observed Slopes of Apsidal Lines in Gabbard Diagram			
Fragments Group	Apogee Line Slope	Perigee Line Slope	Sum of Apsidal Lines Slopes
Group 1 Fragments	93.06 km/min	0.31 km/min	93.38 km/min
Group 2 Fragments	49.07 km/min	45.00 km/min	94.07 km/min
Group 3 Fragments	53.69 km/min	41.38 km/min	95.07 km/min
Group 4 Fragments	56.86 km/min	38.53 km/min	95.39 km/min

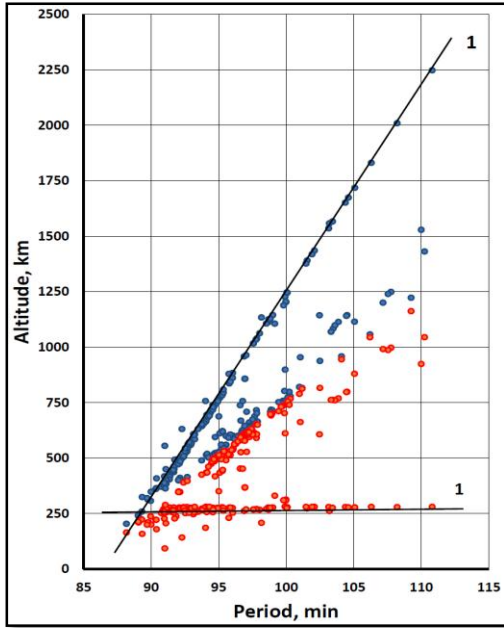


Fig. 1

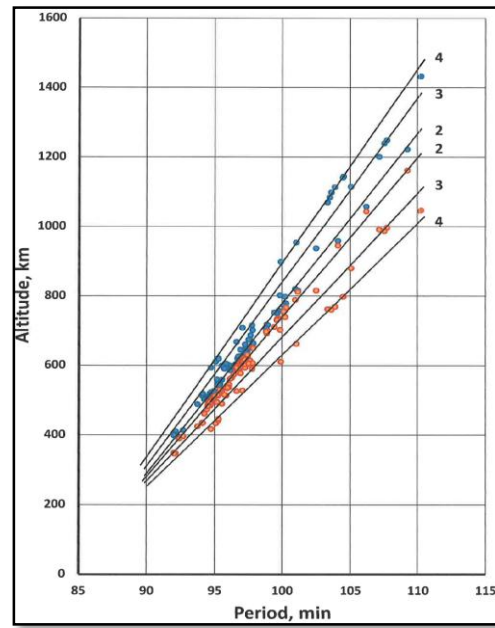


Fig. 2

2. THEORY OF APSIDAL LINES FORMATION ON GABBARD DIAGRAM

The Gabbard diagram of the fragments of a breakup event is a plot of the apogee and perigee heights of the fragments against their orbital time periods. Of the three *orthogonal velocity perturbation components of a fragment* dv_r , dv_d and dv_x in the radial, down-range and cross-range directions respectively, only the first two are relevant in this diagram. The *apogee and perigee lines* in the Gabbard diagram are produced by dv_d s only, with the dv_r s producing departures of the points from these lines [7]. The change in apogee and perigee heights of a fragment, dh_A and dh_P respectively, are given by:

$$dh_A = \frac{1+e}{n} \left[2(1 + e\cos\theta) + \frac{(1-e)\cos\theta(2+e\cos\theta)}{1+e\cos\theta} \right] dv_d \quad (1)$$

and

$$dh_P = \frac{1-e}{n} \left[2(1 + e\cos\theta) - \frac{(1+e)\cos\theta(2+e\cos\theta)}{1+e\cos\theta} \right] dv_d \quad (2)$$

where e is the *eccentricity of the fragmenting orbit*, n the *mean motion* and θ is the *true anomaly*. To evaluate the slopes of the apogee and perigee lines, dh_A/dP and dh_P/dP respectively, in the Gabbard diagram, one needs to convert dv_d to the period P of the fragmenting orbit. This process consists of several steps:

First, for small eccentricities ($e \leq .01$), the **change in energy of a fragment** dE is overwhelmingly due to dv_d [7]:

$$dE = v_d dv_d \quad (3)$$

Second, the change in energy dE is associated with the **change in period** dP :

$$dE = -\frac{2E}{3P} dP \quad (4)$$

Third, the energy of the orbit is:

$$E = -\frac{\mu}{2a} \quad (5)$$

where μ is the **gravitational parameter of the Earth** and a is the **semi-major axis of the fragmenting orbit**.

Fourth, convert the mean motion n into the **orbital time period** P via the defining equation:

$$n = \frac{2\pi}{P} \quad (6)$$

Substituting Eqs. (3) – (6) into Eqs. (1) and (2) and simplifying, we obtain the intermediate forms for the slopes of the apogee and perigee lines:

$$\frac{dh_A}{dP} = \frac{\mu}{6\pi a v_d} (1 + e) \left[2(1 + e \cos \theta) + \frac{(1-e) \cos \theta (2 + e \cos \theta)}{1 + e \cos \theta} \right] \quad (7)$$

and

$$\frac{dh_P}{dP} = \frac{\mu}{6\pi a v_d} (1 - e) \left[2(1 + e \cos \theta) - \frac{(1+e) \cos \theta (2 + e \cos \theta)}{1 + e \cos \theta} \right] \quad (8)$$

Finally, we extricate the θ -dependence in v_d from its expression and the equation of the orbit:

$$v_d = \frac{\sqrt{\mu(1-e^2)}}{r} \quad (9)$$

and

$$r = \frac{a(1-e^2)}{1+e\cos\theta} \quad (10)$$

to obtain:

$$\frac{dh_A}{dP} = \frac{1}{6\pi} \sqrt{\frac{\mu(1-e^2)}{a}} \left[2(1+e) + \frac{(1-e^2)\cos\theta(2+e\cos\theta)}{(1+e\cos\theta)^2} \right] \quad (11)$$

and

$$\frac{dh_P}{dP} = \frac{1}{6\pi} \sqrt{\frac{\mu(1-e^2)}{a}} \left[2(1-e) - \frac{(1-e^2)\cos\theta(2+e\cos\theta)}{(1+e\cos\theta)^2} \right] \quad (12)$$

In Eqs. (9) – (12), r stands for the **radial distance of the fragmentation point from the center of the Earth**.

Summing Eqs. (7) and (8), and simplifying, one gets:

$$\frac{dh_A}{dP} + \frac{dh_P}{dP} = \frac{1}{6\pi} \sqrt{\frac{\mu(1-e^2)}{a}} \quad (13)$$

Eq. (13) implies that the sum of the slopes of the apsidal lines is constant for any orbit of definite size (a) and shape (e) and is independent of the true anomaly θ , where the fragmentation took place. Stated alternatively, we have a **theorem of conservation of slopes of the apsidal lines** which states that **the sum of the slopes of the apsidal lines is constant regardless of where the fragmentation takes places from the same orbit**.

It should be noted that according to Eqs. (11) and (12), the perigee line slope dh_P/dP is minimum when the true anomaly $\theta = 0$. As θ increases, dh_P/dP increases and dh_A/dP decreases. At some point, the two slopes become equal and after that the two lines are interchanged. In general, the angle between the two lines is maximum near the apogee ($\theta = 0$) and perigee ($\theta = \pi$) and zero near $\theta = \pi/2$ and $\theta = 3\pi/2$.

3. BREAKUP JOURNEY OF MICROSAT-R TARGET SATELLITE

Prima facie evidence suggests that Microsat-R, the target satellite of the Indian ASAT experiment, suffered four distinct fragmentations. Immediately prior to the hypervelocity impact with the ASAT, it was found in a nearly circular orbit of eccentricity $e = .0015984$, henceforth called **Orbit 1**. After the collision which produced the Group 1 fragments, the largest remnant, which inherited the identity of the target satellite, was found in a smaller, but slightly more elliptical orbit ($e = .0028309$), now referred to as **Orbit 2**. It is in this orbit that the Microsat-R remnant may well have

undergone three successive explosive breakups caused by the ignition of residual propellants in the satellite, which produced fragment Groups 2, 3 and 4 [5]. After an interval of several days, the Microsat-R remnant was cataloged in **Orbit 3** with the highest apogee height and greatest eccentricity of its lifetime ($e = .0101419$). The relevant orbital parameters of the three reference orbits are listed in Table II, which will prove to be crucial in our following analysis.

Table II. Relevant Pre- and Post-Breakup Orbits of Microsat-R				
Orbit	Epoch, day	Eccentricity	Semi-major axis, km	Period, min
Orbit 1	86.19975	.0015984	6,649.061	89.92904
Orbit 2	86.32379	.0028309	6,645.465	89.85610
Orbit 3	95.00724	.0101419	6,659.421	90.13930

The velocity perturbation components dv_d and dv_r which took Microsat-R from Orbit 1 to Orbit 2 are given, respectively, by [7]:

$$dv_d = \frac{na\sqrt{1-e^2}}{2r} \left(da - \frac{2ae}{1-e^2} de \right) \quad (14)$$

and

$$dv_r = \frac{na^2\sqrt{1-e^2}}{2er^2\sin\theta} \left[2aede - \left(1 - e^2 - \frac{r^2}{a^2} \right) da \right] \quad (15)$$

where n is the mean motion of the fragmenting satellite. In terms of the number of revolutions per day N (loosely called its namesake):

$$n = \frac{2\pi N}{24 \times 60 \times 60} \quad (16)$$

From the value of $N = 16.01262446$ [4], Eq. (16) furnishes: $n = .001164471/\text{s}$. The value of r at the fragmentation point in Orbit 1 is calculated to be 6,659.046431 km [5]. Also, the true anomaly of the target satellite at impact is estimated to be $\theta = 160.0326^\circ$ [5]. The changes in semi-major axis da and eccentricity de from Orbit 1 to Orbit 2 (from Table II) provide: $dv_d = -2.10592$ m/s; and $dv_r = 16.35609$ m/s. These values are qualitatively consistent with the head-on impact with the KKV from below the horizontal plane [5]. As a result of the first breakup of the target satellite by impact, its remnant was found in a smaller and lower orbit (due to retrograde dv_d) with a higher eccentricity (due to positive dv_r).

4. CALCULATED SLOPES OF THE APSIDAL LINES

Since all the relevant quantities in Eqs. (11) and (12) are known for Orbits 1 and 2, the slopes of the apogee and perigee lines of the Group 1 fragments can be calculated directly from these two equations. At the instant of collision, the true anomaly of Microsat-R was 160.0326° and the height of the breakup was 280.9014 km [5]. The results for the Group 1 fragments: $dv_A/dP = 95.76$ km/min; $dv_P/dP = 2.95$ km/min. These values compare favorably with the observed slopes of Group 1 apsidal lines (Table I).

For the explosive breakups from Orbit 2, the true anomaly is unknown. In order to find this, we calculate the change in true anomaly from Orbit 1 to Orbit 2 (cf. [8]):

$$d\theta = \frac{\sqrt{1-e^2}}{nae} \left[\cos\theta dv_r - \sin\theta \left(1 + \frac{1}{1+e\cos\theta} \right) dv_d \right] \quad (17)$$

getting $d\theta = -64.52538^\circ$; whence the true anomaly for Orbit 3: $\theta' = \theta + d\theta = 95.5074^\circ$.

The slopes of the apogee and perigee lines were next calculated for Orbit 2 at intervals of 1° true anomaly. As noted earlier, the slopes depended exclusively on the true anomaly, with their sum remaining constant. Table III covers selected ranges in which the results match with the observed slopes for the Group 2, 3 and 4 lines shown in Table I. By inspection, there were two ranges where this was realized: one for **ascending motion**; and the other for **descending motion** of the fragmenting Microsat-R remnant. For ascending motion, the calculated slopes matched the observed slopes for the Group 2, 3 and 4 lines for true anomalies of 93° , 97° and 101° respectively (marked yellow in Table III); whereas for descending motion, this happened at true anomalies of 273° , 277° and 281° respectively (marked yellow in Table III), at diametrically opposite ends of the orbit. Since the estimated true anomaly for Orbit 2 was 95.5° , it is concluded without any ambiguity that the **explosive fragmentations which produced fragment Groups 2, 3 and 4 must have taken place during the ascending motion of the Microsat-R remnant in Orbit 2**. One can bolster this conclusion from the perturbations of the semi-major axis da and eccentricity de of Orbit 2 prescribed by Lagrange's planetary equations (cf. [8]):

$$da = \frac{2}{n} \left[\frac{e \sin\theta}{\sqrt{1-e^2}} dv_r + \frac{a\sqrt{1-e^2}}{r} dv_d \right] \quad (18)$$

and

$$de = \frac{\sqrt{1-e^2}}{na} \left\{ \sin\theta dv_r + \left[\frac{a(1-e^2)}{er} - \frac{r}{ae} \right] dv_d \right\} \quad (19)$$

Equations (18) and (19) indicate that the effects of dv_r were to increase or decrease both da and de for ascending ($0 < \theta < \pi$) or descending ($\pi < \theta < 2\pi$) motions, respectively.

Table III. Calculated Slopes of Apsidal Lines for Group 2, 3, 4 Fragments				
Sense of Motion	θ , deg	dh_A/dP , km/min	dh_P/dP , km/min	$(dh_A+dh_P)/dP$, km/min
Ascending	92	50.89	47.72	98.61
	93	51.75	46.82	98.61
	94	52.61	45.00	98.61
	95	53.46	45.15	98.61
	96	54.32	44.29	98.61
	97	55.18	43.43	98.61
	98	56.03	42.58	98.61
	99	56.88	41.73	98.61
	100	57.73	40.88	98.61
	101	58.58	40.03	98.61
	102	59.42	39.18	98.61
Descending	272	51.16	47.44	98.61
	273	52.02	46.58	98.61
	274	52.88	45.73	98.61
	275	53.74	44.87	98.61
	276	54.60	44.01	98.61
	277	55.45	43.16	98.61
	278	56.30	42.31	98.61
	279	57.15	41.46	98.61
	280	58.00	40.61	98.61
	281	58.84	39.76	98.61
	282	59.69	38.92	98.61

In fact, the changes are maximum at $\theta = 90^\circ$ and minimum at $\theta = 270^\circ$. *The dramatic increases in both da and de from Orbit 2 to Orbit 3 favor the ascending phase of the remnant's motion.*

As Orbit 2 was still fairly circular ($e = .0022976$) having an orbital period of around 90 min., the 4° intervals between two consecutive explosions translate to **1 min. each for the time intervals**, which means that **the three explosions were over in the space of 2 minutes**. The time interval between the first and second fragmentations, by contrast, as calculated from the epochs of Orbits 1 and 2, translate to 0.12404 d. = 178.62 min. or 2 revolutions. In summary, **the explosive fragmentations which produced fragment Groups 2, 3 and 4 took place at true anomalies of 93° , 97° and 101° respectively in rapid succession of 1 min. intervals after approximately 2 revolutions in the remnant's orbit.**

5. CONCLUSION

Our earlier studies had shed considerable light on various puzzles surrounding the Indian ASAT experiment involving the target satellite Microsat-R [5, 6]. For examples, why was hypervelocity impact not sufficient in explaining the observed debris production; and why explosive fragmentations of the surviving remnant must have taken place in order to explain the observed Gabbard diagram of the fragments. This study reinforces the findings of our earlier studies [5, 6] and gives a plausible chronological scenario of the subsequent explosions consistent with the slopes of the apsidal lines in the Gabbard diagram and pinpoints the locations of the exploding remnant in its breakup orbit.

REFERENCES

- [1] https://wikipedia.org/wiki/Mission_Shakti.
- [2] <https://thediplomat.com/2019/05/why-indias-asat-test-was-reckless>.
- [3] <http://indiandefensenews.in/2019/04/all-you-need-to-know-about-pdv-mk-ii/html>.
- [4] <https://www.space-track.org>.
- [5] A. Tan, R.C. Reynolds & R. Ramachandran, Posthumous analysis of the Indian anti-satellite experiment: Puzzles and Answers, *Adv. Aerospace Sci. Appl.*, 10, 1, 2020.
- [6] A. Tan, R.C. Reynolds & R. Ramachandran, Posthumous analysis of the Indian anti-satellite experiment, Part II: Fragment dispersion study, *Adv. Aerospace Sci. Appl.*, 10, 11, 2020.
- [7] A. Tan & R.C. Reynolds, *Theory of Satellite Fragmentation in Orbit*, World Scientific (2020).
- [8] L. Meirovitch, *Methods of Analytical Dynamics*, McGraw-Hill, New York (1970).

